Applied Mathematics E-Notes, 26(2026), 205-215 ©
Available free at mirror sites of http://www.math.nthu.edu.tw/∼amen/
ISSN 1607-2510

Delving Into The Impact Of Trapezoidal Stenosis On Hemodynamics*

Jeevan Kafle†, Surya Sharma Subedi‡, Pushpa Nidhi Gautam†,‡

Received 8 May 2024

Abstract

Cardiovascular diseases have been recognized as the primary reasons for mortality, mainly because of constricted arteries due to the deposition of foreign particles on the inner wall known as stenosis. The study is focused on the in-depth examination of the blood flow in an artery having trapezoidal-shaped stenosis. The comprehensive evaluation involves studying flow velocity, volumetric flow rate, pressure drop ratio, and shear stress. The analytical solutions obtained are explained graphically for several values of the parameters within the range. The scrutiny is carried out by taking blood as a non-Newtonian fluid, considering the blood flow is steady, axially symmetrical, fully developed, and laminar. Stenosis is concentrated mainly at the narrowest section of the artery, and the wall shear stress is significantly affected by it. The study reveals a reduction in the volumetric flow rate towards the downstream of the trapezoidal stenosis until a plateau phase is achieved. Moreover, the pressure drop and its ratio increase with the elevation of stenotic height, while the blood flow velocity undergoes a rapid decline with minor changes in viscosity. The research initiative of arterial blood flow through trapezoidal-shaped stenosis provides important insights for treating arterial stenosis and its complications.

1 Introduction

Blood, a complex fluid, consists of various suspended blood cells and plasma, the liquid component of blood, which is Newtonian in nature, whereas the suspended blood cells are malleable and display non-Newtonian characteristics [5]. These suspended particles comprise a variety of components such as red blood cells (RBCs) which occupy the largest volume within the blood, making up around 45% of its composition, white blood cells (WBCs), platelets, proteins, other organic molecules, and salts, each playing an important role in various physiological processes [2]. Understanding the circulatory system necessitates an exploration of blood flow across different stenotic configurations and the dynamics of fluidic variables become pivotal as stenosis progresses, resulting in significant alterations to blood flow and ultimately culminating in cardiovascular ailments [4]. The deposition of cholesterol, lipid particles, and other exogenous particles results in the formation of atherosclerotic plaque known as stenosis, while abnormal tissue growth also contributes to stenosis [18]. Various morphological shapes of stenosis consist of symmetrical, triangular, trapezoidal, bell-shaped, rectangular, and composite [19]. Each type of stenosis impedes blood flow and diminishes blood supply, posing challenges to the circulatory system [22]. Exceedingly high shear stress near the stenosis neck may entirely block the passage of blood to the heart, thereby disrupting the cardiovascular system [18]. The analysis and interpretation of issues regarding arterial blood flow through trapezoidal-shaped stenosis offer valuable insights into stenotic regions, thus enabling the development of effective treatment strategies aimed at addressing arterial stenosis and its associated complications.

Young [22] was a pioneer in analyzing how blood flows in a narrowed artery using mathematical equations, focusing on a simplified model with axial symmetry and no radial velocity components. Fry [7], highlighted the pivotal role of wall shear stress in arterial disease progression. Halder [9], conducted a thorough analysis

*Mathematics Subject Classifications: 20F05, 20F10, 20F55, 68Q42.
†Central Department of Mathematics, Institute of Science and Technology, Tribhuvan University, Nepal
‡Department of Mathematics, Patan Multiple Campus, Tribhuvan University, Nepal

of blood flow within narrow regions of different shapes, emphasizing how these narrow areas impact the resistance to flow in the artery segment. Azuma and Fukushima [1], utilized constricted vessels to generate the flow patterns. MacDonald [17], analyzed the impact of uniformity on cylinder-shaped design constriction. The blood flow issue for an artery stenotic area was theoretically addressed by Chakravarty and Mandal [3]. Kafle et al. [12], embarked on a creative exploration into the world of hemodynamic variables as blood flows through an artery. Gautam et al. [8], elucidate the impact of progressive stenosis on hemodynamics over time, to rectify the resulting disadvantage while maintaining the symmetrical shaped stenosis and blood as a non-Newtonian fluid. Tang et al. [21], considered both symmetric and asymmetric-shaped stenoses while examining the blood flow inside the carotid artery. Kafle et al. [11], also delved into this subject matter in their research. The configuration and size of stenosis significantly influence flow dynamics within cylindrical arteries, as evidenced by Lorenzini and Casalena [15], who found that trapezoidal plaque shapes pose the most severe pathology, promoting increased strain and heightened deposition risks along artery walls. Dada et al. [6], have studied the blood flow through a tapered overlapping stenosed artery with a porous wall and concluded that the increase in Darcy number reduces flow resistance in the unobstructed region of the artery. Subedi et al. [20] have explored the enigma of blood circulation through a trapezoidal narrowing on two-layered blood flow model. Jabbar et al. [10], conducted a numerical examination of pulsatile blood flow around diverse plaque forms, including trapezoidal, elliptical, and triangular. Keshavarz and Kadem,. and Liu [14, 16], studied pulsed blood passage in curved arteries with different levels of stenosis, exploring the impact of spiral blood flow within constricted arteries. Kamanger et al. [13], studied blood flow dynamics under several geometries, including trapezium, triangular, and elliptical forms, in response to the severity of obstruction. Their investigation covered various sizes of stenosis, and found that trapezoidal geometries have higher wall shear stress than triangular and elliptical shapes. That is why trapezoidal stenosis is a more vulnerable problem.

A lot of research has been conducted in recent decades to examine blood flow in stenotic arteries, but there is still a significant gap in understanding the impact of trapezoidal form stenosis on arterial blood flow, motivating us for our study. Consequently, the present study prompts us to explore the impact of trapezoidal-shaped stenosis on blood flow dynamics. In this work, we examine how blood flow parameters are affected by trapezoidal-shaped stenosis. Effectively, we use a model for the trapezoidal shape to address this problem. After obtaining solutions, the velocity profile, volumetric flow rate, shear stress, and pressure drop are examined. It is assumed in this mathematical model that the flow in the stenosed section of an artery is axisymmetric and laminar.

1.1 Blood Flow Model for Trapezoidal Shaped Stenosis

Considering the constant blood flow in a stenosed artery which is equilateral in axial direction, let R_0 and R stand for the respective radii of the stenosis-free and stenosis-filled arteries. The artery is viewed as a circular, inelastic tube where the radial blood flow is disregarded. It has been proposed that only the axial direction of blood flow occurs. Additionally, we consider the drift to be completely formed.

1.2 The Geometry and the Rate of Blood Flow Through Trapezoidal Stenosis.

The wall shear stress is defined as,

$$\tau = -\mu \left(\frac{dv}{dr} \right)^{\frac{1}{n}} \tag{1}$$

where v is the blood velocity, which is a function of r, and r is varying radius from 0 to R, n is power law index for non-Newtonian fluid and μ is its viscosity. The shear stress formula may be expressed as a function of pressure as

$$\tau = \frac{Pr}{2}. \tag{2}$$

The pressure gradient $\frac{-\partial p}{\partial z}$ is denoted by P. From equation (1) and equation (2) we get

$$\frac{dv}{dr} = \left(\frac{Pr}{2\mu}\right)^{\frac{1}{n}} \tag{3}$$

and after integrating (3) from r to R, yields

$$v = \left(\frac{P}{2\mu}\right)^{\frac{1}{n}} \frac{n}{n+1}\left(R^{1+\frac{1}{n}} - r^{1+\frac{1}{n}}\right). \tag{4}$$

Velocity is zero at the wall of the artery and is maximum at the center for $r = 0$. Given that blood is identified as non-Newtonian, the power law index (n) for blood ranges from $0.68 \leq n \leq 0.8$, and we have taken $n = 0.75$ as an average value, and the shape of the stenosis is specified as [19],

$$\frac{R}{R_0} = \begin{cases} 1 - \frac{4\delta}{R_0^2}(z-d), & \text{if} \quad d \leq z \leq d + \frac{L_0}{4}, \\ 1 - \frac{\delta L_0}{R_0^2}, & \text{if} \quad d + \frac{L_0}{4} \leq z \leq d + \frac{3L_0}{4}, \\ 1 - \frac{2\delta}{R_0^2}(L_0 - 2(z - d - \frac{L_0}{2})), & \text{if} \quad d + \frac{3L_0}{4} \leq z \leq d + L_0, \\ 1, & \text{otherwise.} \end{cases} \tag{5}$$

In the domain of the Stenotic area, the parameter d serves as the point of origin, denoted by δ (mm) to represent the magnitude of the Stenotic region, while L_0 (mm) stands for the longitudinal extent of the Stenotic area, where z smoothly varies from 0 to L_0.

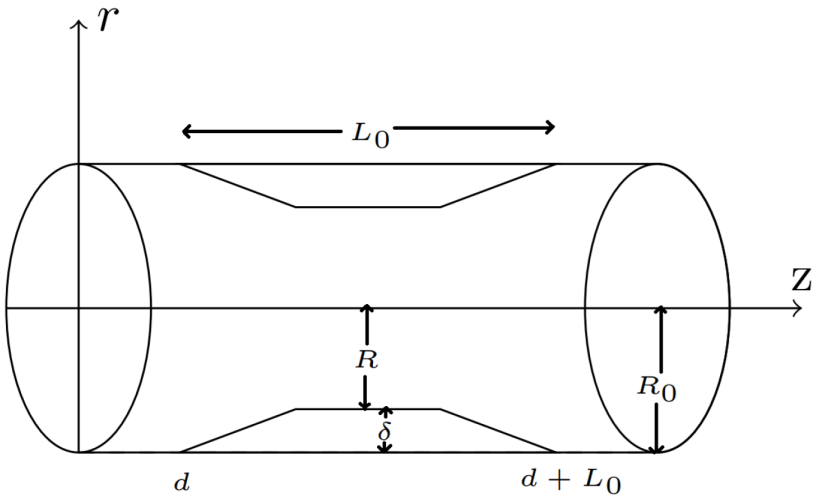

Figure 1: Part of the artery with stenosis.

If $d = 0$ then our geometry changes as

$$\frac{R}{R_0} = \begin{cases} 1 - \frac{4\delta}{R_0^2}(z), & \text{if} \quad 0 \leq z \leq \frac{L_0}{4}, \\ 1 - \frac{\delta L_0}{R_0^2}, & \text{if} \quad \frac{L_0}{4} \leq z \leq \frac{3L_0}{4}, \\ 1 - \frac{4\delta}{R_0^2}(L_0 - z), & \text{if} \quad \frac{3L_0}{4} \leq z \leq L_0, \\ 1, & \text{otherwise.} \end{cases} \tag{6}$$

Now from (4) we have

$$v = \left(\frac{P}{2\mu}\right)^{\frac{1}{n}} \frac{n}{n+1} R_0^{1+\frac{1}{n}} \left(\left(\frac{R}{R_0}\right)^{1+\frac{1}{n}} - \left(\frac{r}{R_0}\right)^{1+\frac{1}{n}}\right). \tag{7}$$

By replacing $\frac{R}{R_0}$ in equation (6) with the formula in equation (7), we obtain

$$v = \left(\frac{P}{2\mu}\right)^{\frac{1}{n}} \frac{n}{n+1} R_0^{1+\frac{1}{n}} \begin{cases} -\left(\frac{r}{R_0}\right)^{\frac{n+1}{n}} + \left(1 - \frac{4\delta}{R_0^2} z\right)^{\frac{n+1}{n}}, & \text{if} \quad 0 \le z \le \frac{L_0}{4}, \\ -\left(\frac{r}{R_0}\right)^{\frac{n+1}{n}} + \left(1 - \frac{\delta L_0}{R_0^2}\right)^{\frac{n+1}{n}}, & \text{if} \quad \frac{L_0}{4} \le z \le \frac{3L_0}{4}, \\ -\left(\frac{r}{R_0}\right)^{\frac{n+1}{n}} + \left(1 - \frac{4\delta}{R_0^2}(L_0 - z)\right)^{\frac{n+1}{n}}, & \text{if} \quad \frac{3L_0}{4} \le z \le L_0. \end{cases} \tag{8}$$

1.3 Volumetric Flow Rate

To calculate the volumetric flow rate Q, we use

$$Q = 2\pi \int_0^R v r dr. \tag{9}$$

After substituting the expression for v from (4) and integrating,

$$Q = \frac{n\pi}{3n+1} \left(\frac{P}{2\mu}\right)^{\frac{1}{n}} R_0^{\frac{3n+1}{n}} \left(\frac{R}{R_0}\right)^{\frac{3n+1}{n}}. \tag{10}$$

Putting the value of $\frac{R}{R_0}$ from (6) and applying binomial expansion up to two terms,

$$Q = \left(\frac{P}{2\mu}\right)^{\frac{1}{n}} \frac{n\pi}{3n+1} R_0^{\frac{3n+1}{n}} \begin{cases} \left(1 - \frac{4\delta}{R_0^2} z\right)^{\frac{3n+1}{n}}, & \text{if} \quad 0 \le z \le \frac{L_0}{4}, \\ \left(1 - \frac{\delta L_0}{R_0^2}\right)^{\frac{3n+1}{n}}, & \text{if} \quad \frac{L_0}{4} \le z \le \frac{3L_0}{4}, \\ \left(1 - \frac{4\delta}{R_0^2}(L_0 - z)\right)^{\frac{3n+1}{n}}, & \text{if} \quad \frac{3L_0}{4} \le z \le L_0, \\ 1, & \text{otherwise.} \end{cases} \tag{11}$$

This particular relation (11) serves as a clear indication of the volumetric flow rate.

1.4 Pressure Drop

Equation (10) gives us

$$P = \frac{2\mu Q^n}{R_0^{3n+1}} \left(\frac{3n+1}{n\pi}\right)^n \left(\frac{R}{R_0}\right)^{-(3n+1)}.$$

After the blood flows through the stenosis, the pressure drop ΔP is measured and is found to be

$$\Delta P = \int_0^{L_0} \frac{2\mu Q^n}{R_0^{3n+1}} \left(\frac{3n+1}{n\pi}\right)^n \left(\frac{R}{R_0}\right)^{-(3n+1)} dz.$$

Substituting the value of R/R_0 and performing a binomial expansion up to two terms. As our function is a piece-wise continuous function. So we write,

$$\Delta P = \Delta P_1 + \Delta P_2 + \Delta P_3, \tag{12}$$

where

$$\Delta P_1 = \frac{2\mu Q^n}{R_0^{3n+1}} \left(\frac{3n+1}{n\pi}\right)^n \left(\frac{L_0}{4} + (3n+1)\frac{4\delta}{R_0^2}\frac{L_0^2}{32} + \frac{(3n+1)(3n+2)}{2}\left(\frac{4\delta}{R_0^2}\right)^2 \frac{L_0^3}{192}\right), \tag{13}$$

$$\Delta P_2 = \frac{2\mu Q^n}{R_0^{3n+1}} \left(\frac{3n+1}{n\pi}\right)^n \left[1 + (3n+1)\left(\frac{\delta L_0}{R_0^2}\right) + \frac{(3n+1)(3n+2)}{2}\left(\frac{\delta L_0}{R_0^2}\right)^2\right] \frac{L_0}{2}, \tag{14}$$

$$\Delta P_3 = \frac{2\mu Q^n}{R_0^{3n+1}} \left(\frac{3n+1}{n\pi}\right)^n \left(\frac{L_0}{4} + (3n+1)\,\frac{4\delta}{R_0^2}\frac{L_0^2}{32} + \frac{(3n+1)\,(3n+2)}{2}\left(\frac{4\delta}{R_0^2}\right)^2 \frac{L_0^3}{192}\right). \tag{15}$$

From equation (12)–(15),

$$\Delta P = \frac{2\mu Q^n}{R_0^{3n+1}} \left(\frac{3n+1}{n\pi}\right) \left(L_o + (3n+1)\,\frac{4\delta}{R_0^2}\frac{9L_0^2}{16} + \frac{(3n+1)\,(3n+2)}{2}\left(\frac{4\delta}{R_0^2}\right)^2 \frac{4L_0^3}{96}\right). \tag{16}$$

Now for ΔP_0, we take $\delta = 0$ on equation (16), which gives

$$\Delta P_0 = \frac{2\mu Q^n}{R_0^{3n+1}} \left(\frac{3n+1}{n\pi}\right)^n L_0.$$

The pressure drop ratio can be effectively articulated as,

$$\frac{\Delta P}{\Delta P_0} = 1 + (3n+1)\,\frac{4\delta}{R_0^2}\frac{9L_0}{16} + \frac{(3n+1)\,(3n+2)}{2}\left(\frac{4\delta}{R_0^2}\right)^2 \frac{4L_0^2}{96}.$$

1.5 Shear Stress and the Ratio of the Greatest to the Smallest Shear Stress

It makes sense that the shear stress at the stenosis wall would be considered small, given its greater proximity to the center. Similarly, the normal artery's (without stenosis) wall experiences the greatest shear stress due to its greatest distance from the artery's center, which is specifically defined as such

$$\tau_{min} = \frac{PR}{2}, \qquad \tau_{max} = \frac{PR_0}{2}.$$

Therefore, the shear stress ratio is presented as

$$\frac{\tau_{max}}{\tau_{min}} = \left(\frac{R_0}{R}\right) = \left(\frac{R}{R_0}\right)^{-1}.$$

2 Result and Discussion

The stenosis having a trapezoidal shape has been specifically designed and used to examine various characteristics and aspects of blood circulation within an artery affected by it, providing valuable insights into the dynamics of this common vascular condition. Cogent solutions of the celerity profile, volumetric flow rate, pressure drop, shear stress, and viscosity on the above-mentioned aspects are scrutinized. The pressure recorded is 100 mmHg, with the artery's radius measured at 0.3 mm, a blockage of 75% is taken into account, and the value of n is assumed to be 0.75 as an average if not specified.

2.1 The Velocity Account of Blood Flow Through a Narrowed Artery

In Figure 2(a), an artery of radius 0.3 mm is considered to measure the velocity at the center. Numerical values of the velocity for the viscosity 3.5 cP, 4 cP, 4.5 cP, and 5 cP are 0.895 mm/s, 0.7491 mm/s, 0.6402 mm/s, and 0.5563 mm/s respectively at the center considering pressure 100 mm of Hg. The parabolic-shaped curves are obtained when we vary the radius (r) from -0.3 mm to 0.3 mm. In the artery's inner wall, the velocity is zero and increases gradually towards the center. The speed increases by 0.0839 mm/s at the center when the viscosity decreases from 5 cP to 4.5 cP. Similarly, when the viscosity drops from 4.5 cP to 4 cP and 4 cP to 3.5 cP, respectively, an increment of 0.1089 mm/s and 0.1459 mm/s is seen. Totaling a 0.3387 mm/s rise in velocity when the viscosity decreases from 5 cP to 3.5 cP. However, the augmentation in velocity is more and more for decreasing viscosity. Ultimately, it is concluded that the viscosity and velocity of blood are inversely related. Table 1 from Figure 2(b) presents findings on the correlation between velocity

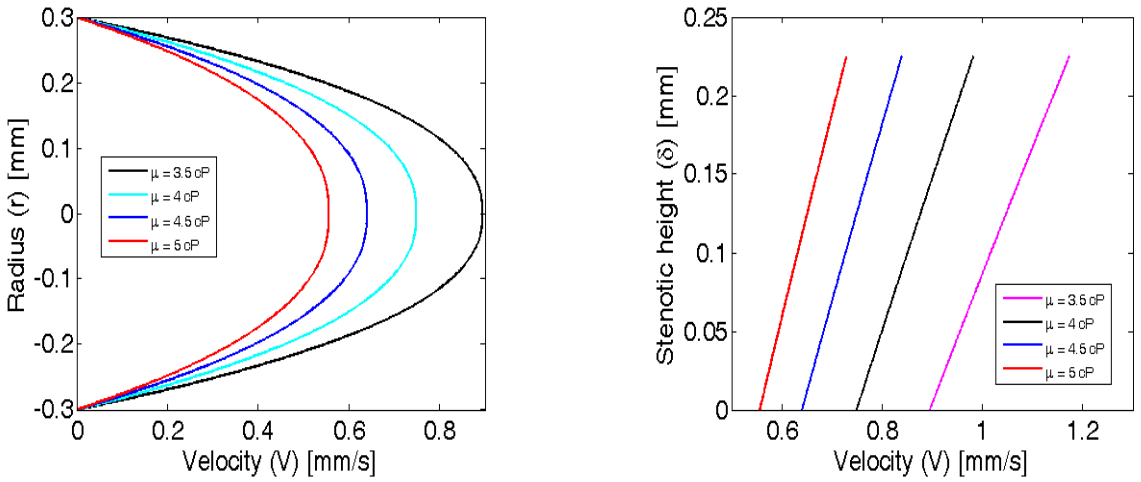

(a) (b)

Figure 2: (a)**:** Velocity (V) vs Radius (r) for different viscosity, (b)**:** Variation of velocity with stenotic height.

and stenotic height in arteries. In the absence of stenosis for an artery of 0.3 mm, the velocities are recorded as 0.8962 mm/s, 0.7491 mm/s, 0.6402 mm/s, and 0.5563 mm/s for viscosity values of 3.5 cP, 4 cP, 4.5 cP, and 5 cP, respectively. When an artery has a stenosis height of 0.225 mm which is 75% blockage of the mesa section, the velocities are observed to be 1.173 mm/s, 0.9818 mm/s, 0.8391 mm/s, and 0.7292 mm/s for viscosity values of 3.5 cP, 4 cP, 4.5 cP, and 5 cP, respectively. This indicates a 30.8859%, 31.06394%, 31.06841%, and 31.0803% increase in velocity for respective viscosity. All of the above studies illustrate that an increase in stenotic height is linked to higher velocities.

Index	Viscosity (μ) [cP]	Velocity (V) [mm/s]						
i	μ/δ	0mm	0.05mm	0.10mm	0.125mm	0.15mm	0.20mm	0.225mm
1	3.5 cP	0.89620	0.95520	1.01600	1.04700	1.07800	1.14100	1.17300
2	4.0 cP	0.74910	0.79940	0.85050	0.87640	0.90250	0.0.95520	0.98180
3	4.5 cP	0.64020	0.68320	0.72700	0.74910	0.77130	0.81640	0.83910
4	5.0 cP	0.55630	0.59370	0.63170	0.65090	0.67020	0.70940	0.72920

Table 1: Velocity at varying stenotic height for different viscosity.

2.2 The Volumetric Flow Rate of Blood Flow via a Stenotic Artery

Figure 3(a) depicts the impact of viscosity on the volumetric flow rate. The outcome reveals viscosity and volumetric flow rate exhibit an inverse relationship. For viscosity values of 5 cP, 4.5 cP, 4 cP, and 3.5 cP, corresponding values for the volumetric flow rate are 0.07 mm^3/s, 0.9 mm^3/s, 0.11 mm^3/s, 0.13 mm^3/s, respectively for an artery of 0.3 mm. Similarly, the volumetric flow rates are 0.0146 mm^3/s, 0.0168 mm^3/s, 0.0197mm^3/s, 0.0235 mm^3/s, respectively for an artery of 0.2 mm. As the radius decreases, the volumetric flow rate decreases in a parabolic manner, resulting in only a small amount of blood flow in a tiny artery. It turned out that fluids with higher viscosity often have lower flow velocities, resulting in fewer fluids moving through when compared to fluids with lower viscosity. Therefore, it can be deduced that fluids possessing increased viscosity generally display a decreased volumetric flow rate. It is crystal clear in the Figure 3(a). Similarly, in Figure 3(b) volumetric flow rate vs axial width is plotted for various amounts of viscosity. When

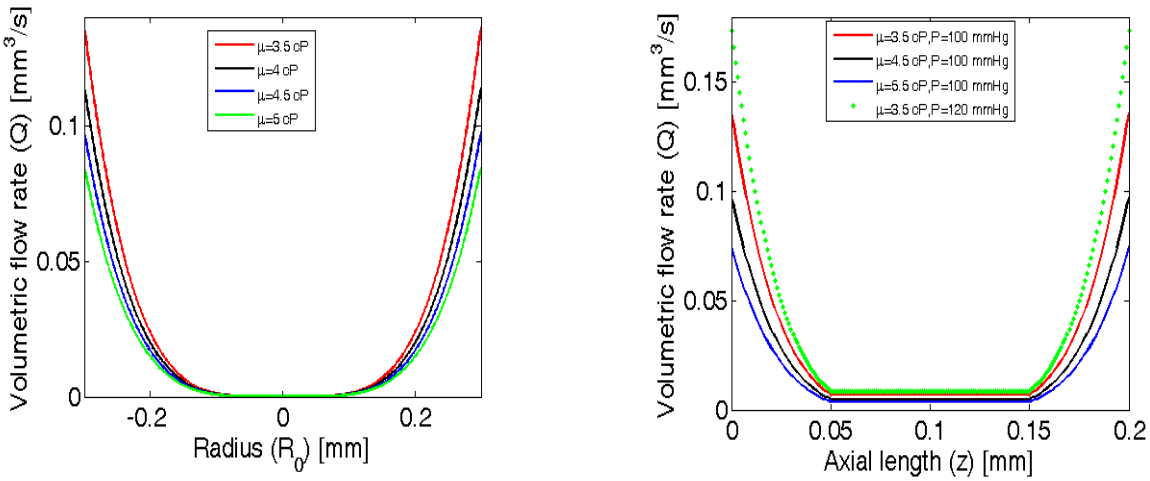

(a) (b)

Figure 3: (a)**:** Volumetric flow of blood via a stenotic artery with a different radius for varying viscosity, (b)**:** Volumetric flow of blood via a stenotic artery for varying viscosity along the stenotic length.

$P = 100$ mm of Hg maximum possible volumetric flow rate is 0.13 mm^3/s, whereas for $P = 120$ mm of Hg maximum possible volumetric flow rate is 0.17 mm^3/s for the same amount of viscosity $\mu = 3.5$ cP. This shows that an increase in pressure causes an increase in volumetric flow rate which is obvious and can be visualized from Figure 3(b). However the volumetric flow rate decreases until it reaches the mesa and remains constant with the values 0.00676 mm^3/s, 0.004835 mm^3/s, 0.0037 mm^3/s for respective viscosity 3.5 cP, 4 cP, 4.5 cP till the end of the mesa, then it starts to increase again as illustrated in Figure 3(b). We may state that a rise in pressure causes a rise in the volumetric flow rate in collocation. Proceeding axially until the plateau volumetric flow rate falls and stays constant, then progressively rising if a constant pressure of 100 mm of Hg is taken into account all over the stenosis.

Index	Viscosity [cP]	Volumetric Flow Rate (Q) $[mm^3/s]$					Ratio
i	μ/z	0mm	0.02mm	(0.05-0.15)mm	0.18mm	0.20mm	$Q_{\min}/Q_0$
1	3.5	0.13630	0.05181	0.00676	0.05181	0.13630	0.04960
2	4.0	0.09747	0.037060	0.00484	0.03706	0.09747	0.04960
3	4.5	0.07459	0.02836	0.00370	0.02836	0.07459	0.04960

Table 2: Volumetric flow rate at various locations within a stenosis under varying viscosities at different points along the stenosis.

For 0.65, 0.75, 0.85, 1 values of power law index (n) corresponding approximations for the maximum possible volumetric flow rate are 0.09 mm^3/s, 0.11 mm^3/s, 0.13 mm^3/s, 0.17 mm^3/s, accordingly. Assuming constant pressure throughout the stenosis, the volumetric flow rate in the above scenario falls axially until it reaches a plateau with flow rates of 0.007546 mm^3/s, 0.00676 mm^3/s, 0.006223 mm^3/s, and 0.00568 mm^3/s at 3.5 cP viscosity. The volumetric flow rate increases downstream from the right endpoint of the mesa. The preceding Figure 4(a) and findings show that the power law index and volumetric flow rate have an inverse relationship.

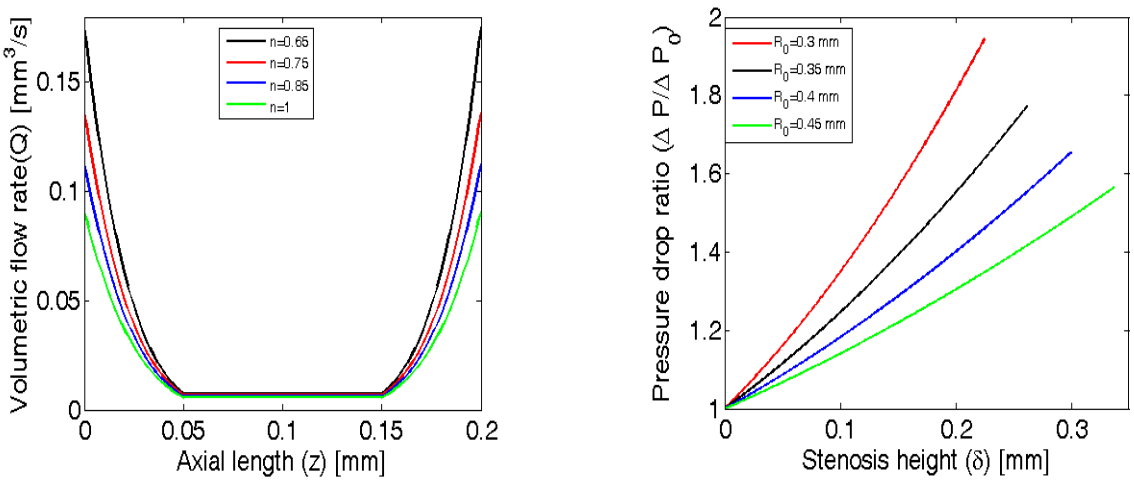

(a) (b)

Figure 4: (a)**:** Volumetric flow of blood via a stenotic artery for varying power law index, (b)**:** Pressure drop and its ratio across stenotic artery.

2.3 Pressure Drop and its Ratio Across Stenotic Artery

As narrated in Figure 4(b) comparison is made regarding the ratio of pressure drop to the thickness of the stenosis across various radii. The radii observed, specifically R_0 with measurements of 0.3 mm, 0.35 mm, 0.4 mm, and 0.45 mm, with stenosis height of 0.2 mm, the corresponding pressure drop ratios are recorded as 1.81, 1.551, 1.402, and 1.304 respectively. This indicates a notable increase in pressure by 81%, 55.1%, 40.2%, and 30.4% as one transitions from an artery without stenosis to an artery with a stenosis height of 0.2 mm. Furthermore, when the blockage reaches 75%, the pressure drop ratios escalate to 1.944, 1.772, 1.654, and 1.564 for the corresponding radii, reinforcing the trend of heightened pressure with increased stenosis height. In a scenario where a stenosis obstructs 75% of the lumen in an artery with a radius of 0.3 mm, the resulting increase in pressure is measured at 94.4%. Analogously, in arteries measuring 0.35 mm, 0.4 mm, and 0.45 mm, radius, the corresponding pressure elevations are 77.2%, 65.4%, and 56.4%, respectively, under the condition of a 75% blockage. The findings strongly suggest that as the stenosis height rises, there is a clear elevation in pressure, with a notable inverse correlation between radius size and pressure levels. This relationship underscores the importance of considering both stenosis characteristics and vessel dimensions when assessing pressure variations in arterial flow.

2.4 Shear Stress and the Ratio of the Greatest to the Smallest Shear Stress

In Figure 5(a) initially, the ratio is 1 in the absence of stenosis. Following an increase in stenosis height to 0.15 mm, the shear stress ratio exhibits values of 1.174, 1.231, 1.324, 1.500, and 1.923 for radii of 0.45 mm, 0.40 mm, 0.35 mm, 0.30 mm, and 0.25 mm correspondingly, indicating a respective increase of 17.4%, 23.1%, 32.4%, 50%, and 92.3% in shear stress. Moreover, when introducing a 75% blockage, the shear stress ratio escalates significantly to 1.499, 1.600, 1.748, 2.000, and 2.490. These findings suggest that as the radius of the stenosis decreases, the proportional escalation in shear stress increases gradually. Furthermore, there is a consistent gradual increase in shear stress with the elevation of stenosis height. The shear stress rises with stenosis height, causing more blockage and subsequently higher shear stress levels within the system. Notably, the shear force experiences a doubling effect at the maximum percentage of blockage for radii that are less than or equal to 0.3 mm, indicating a significant risk of rupture in that specific region. The illustration depicted in Figure 5(b) along with the data provided in Table 3 visually showcases the correlation between

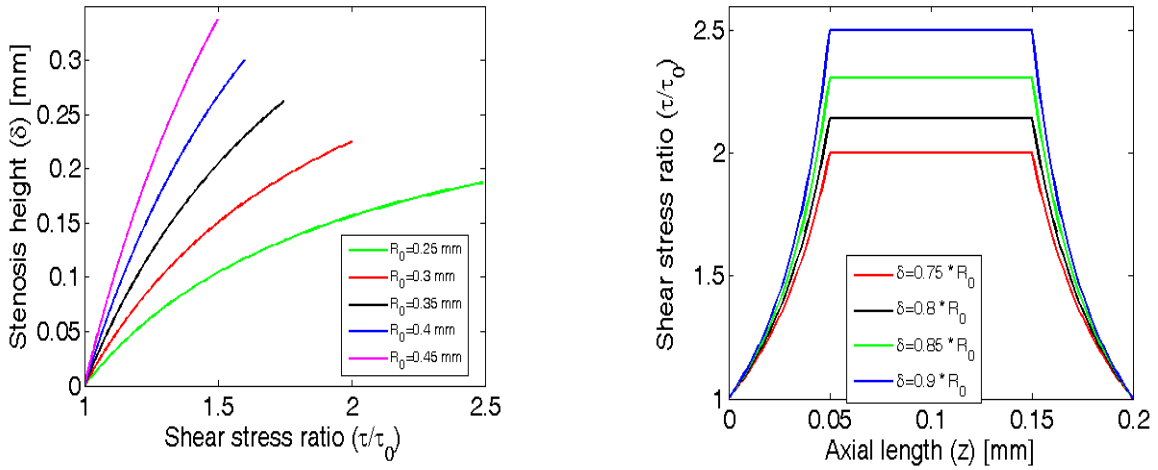

(a) (b)

Figure 5: (a)**:** Effect of stenosis on shear stress ratio, (b)**:** Impact of stenosis on shear stress ratio for varying percentage of blockage.

Index	Blockage percent	Shear stress ratio ($\frac{\tau_{max}}{\tau_{min}}$)						
i	δ/z	0mm	0.02mm	0.04mm	(0.05-0.15)mm	0.16mm	0.18mm	0.20mm
1	$0.75 * R_0$	1.000	1.250	1.667	2.000	1.250	1.667	1.000
2	$0.80 * R_0$	1.000	1.271	1.744	2.143	1.744	1.271	1.000
3	$0.85 * R_0$	1.000	1.293	1.829	2.308	1.829	1.293	1.000
4	$0.90 * R_0$	1.000	1.316	1.923	2.500	1.316	1.923	1.000

Table 3: Shear stress ratio at various locations within a stenosis under varying blockage percentages.

the ratio of maximum and minimum shear forces at the different points of stenosis. This representation is based on a scenario where the total length of stenosis is 0.2 mm in arteries with identical radii of 0.3 mm but varying levels of blockage, adding a layer of complexity to the analysis. Initially, the shear force ratio is one, establishing a baseline for comparison. At the point 0.02 mm from the beginning of the stenosis origin, the shear stress ratio progressively rises to 1.25, 1.271, 1.293, and 1.316 for artery with blockages of 75%, 80%, 85%, and 90% respectively, showcasing the impact of blockage on shear forces. Upon advancing to 0.04 mm, the ratio spikes further to 1.667, 1.744, 1.829, and 1.923 for the corresponding blockage percentages, reflecting the escalating nature of this relationship. Transitioning into the mesa section, the shear force ratio reaches its peak 2.000, 2.143, 2.308, and 2.500, signifying a substantial surge of 100% or more in shear force within the mesa area compared to the non-stenotic segment, highlighting a critical vulnerability in the system. Consequently, as one navigates from the end of the mesa region towards the end of the stenosis, there is a gradual decrease in the shear stress ratio, indicating a diminishing trend in shear forces along this trajectory, emphasizing the dynamic nature of the system. In conclusion, this analysis implies that the higher the blockage percentage, the higher the shear stress ratio, underscoring the importance of considering blockage levels in assessing shear forces in stenotic arteries.

3 Summary

Atherosclerotic plaque, or stenosis, is created when cholesterol, lipid particles, and other foreign particles are deposited or anomalous growth of tissues occurs in the inner wall of an artery which affects the hemody-

namics. Trapezoidal-shaped stenosis plays a significant role in hemodynamics due to excessively increasing shear stress at the neck of the stenosis. The velocity profile, pressure drop, shear stress, and volumetric flow rate in an artery with trapezoidal-shaped stenosis are examined using Navier Stokes equations. Various degrees of stenosis have been considered to observe their impact on the aforementioned attributes. It has been noted that the velocity decreases gradually for increasing viscosity and there is a positive correlation between stenosis height and velocity. Furthermore, the volumetric flow rate experiences a significant decrease as viscosity escalates, doubling when the viscosity decreases by 1.5 cP within the range. However, regardless of the viscosity, the ratio between the lowest and highest volumetric flow rate stays constant. Additionally, blood flow velocity falls promptly with even a minor increase in viscosity, and the highest velocity is reached at the flat part (maximum height) of trapezoidal-shaped stenosis. Shear force nearly doubles in the mesa section of trapezoidal stenosis, creating a dangerous scenario that may lead to the rupture of the arterial wall. These research findings offer a valuable contribution towards comprehending the hemodynamic abnormalities associated with trapezoidal stenosis, and it may also aid in the development and enhancement of highly sensitive tools for diagnosis and treatment.

Acknowledgement. Jeevan Kafle acknowledges the Research Directorate, Rector's Office, Tribhuvan University, Kathmandu, Nepal, for the financial support through the Major Research Grant.

References

[1] T. Azuma and T. Fukushima, Flow patterns in stenotic blood vessel models, Biorheology, 13(1976), 337–355.

[2] J. R. Batten and R. M. Nerem, Model study of flow in curved and planar arterial bifurcations, Cardiovascular research, 16(1982), 178–186.

[3] S. Chakravarty, Effects of stenosis on the flow-behaviour of blood in an artery, International Journal of Engineering Science, 16(1982), 175–180.

[4] S. Charm and G. Kurland, Viscometry of human blood for shear rates of 0–100,000 sec-1, Nature, 206(1965), 617–618.

[5] K. Crawford, K. Jakub, J. S. Lockhart and J. L. Wold, Knowledge, attitudes, and beliefs of cardiovascular disease prevention in young adults in the country of Georgia, Journal of Nursing Scholarship, 5(2023), 903–913.

[6] M. S. Dada, A. J. Babatunde and M. M. Tunde, Fluid analysis of double-layered blood flow through a tapered overlapping stenosed artery with a porous wall, Journal of Heat and Mass Transfer Research, 9(2022), 189–196.

[7] D. L. Fry, Responses of the arterial wall to certain physical factors, Ciba Foundation Symposium 12-atherogenesis: initiating factors, 12(1973), 93–125.

[8] P. N. Gautam, C. Pokharel, G. R. Phaijoo, P. Kattel and J. Kafle, Effect of increasing stenosis over time on hemodynamics, Biomath, 12(2023), 2310067–2310067.

[9] K. Haldar, Effects of the shape of stenosis on the resistance to blood flow through an artery, Bulletin of Mathematical Biology, 47(1985), 545–550.

[10] U. I. A. Jabbar, R. U. Ali, P. Khalid and U. H. K. Niazi, Three-dimensional numerical analysis of pulsatile blood flow around different plaque shapes in human carotid artery, International Journal of Bioscience, Biochemistry and Bioinformatics, 2(2012), 305.

[11] J. Kafle, H. P. Gaire, and P. Kattel, Analysis of blood flow through curved artery with mild stenosis, Mathematical Modeling and Computing, 9(2022), 217–225.

[12] J. Kafle, K. Panta, P. N. Gautam and C. Pokharel, Mathematical analysis of hemodynamic parameters of blood flow in an artery, Mathematics Education Forum Chitwan, 7(2022), 82–91.

[13] S. Kamangar, I. A. Badruddin, N. A. Ahamad, K. Govindaraju,N. Nik-Ghazali, N. J. Ahmed and T., M. Khan, The influence of geometrical shapes of stenosis on the blood flow in stenosed artery, Sains Malaysiana, 46(2017), 1923–1933.

[14] Z. Keshavarz-Motamed and L. Kadem, 3d pulsatile flow in a curved tube with coexisting model of aortic stenosis and coarctation of the aorta, Medical engineering & physics, 33(2011), 315–324.

[15] G. Lorenzini and E. Casalena , Cfd analysis of pulsatile blood flow in an atherosclerotic human artery with eccentric plaques, Journal of biomechanics, 41(2008), 1862–1870.

[16] B. Liu, The influences of stenosis on the downstream flow pattern in curved arteries, Medical & engineering physics, 29(2007), 868–876.

[17] D. A. MacDonald, On steady flow through modelled vascular stenoses, Journal of biomechanics, 12(1997), 13–20.

[18] V. A. Nosovitsky, O. J. Ilegbusi, J. Jiang and C. L. Feldman, P. H. Stone, Effects of curvature and stenosis-like narrowing on wall shear stress in a coronary artery model with phasic flow, Computers and Biomedical Research, 30(1997), 61–82.

[19] R. Ponalagusamy and R. Manchi, A study on two-layered (K.L-Newtonian) model of blood flow in an artery with six types of mild stenoses, Appl. Math. Comput., 367(2020), 124767, 22 pp.

[20] S. Sh. Subed, P. N. Gautam, and J. Kafle, Analysis of hemodynamic impacts on two-layer blood flow in a trapezoidal stenosis within an artery, Eurasian journal of Mathematical and Computer Applications, 3(2025) 97–111.

[21] D. Tang, C. Yang and D. N. Ku, A 3-d thin-wall model with fluid-structure interactions for blood flow in carotid arteries with symmetric and asymmetric stenoses, Computers & Structures, 72(1999), 357–377.

[22] D. F. Young, Effect of time-dependent stenosis on flow through a tube, J. Eng. Ind., 90(1968), 248–254.